Image Cover Sheet

CLASSIFICATION	SYSTEM NUMBER
UNCLASSIFIED	511561

TITLE

Nonlocal Boundary Conditions for Finite-Difference Parabolic Equation Solvers

System Number:

Patron Number:

Requester:

Notes:

DSIS Use only:

Deliver to:

Non-local boundary conditions for finite-difference PE solvers

David Yevick.
Department of Electrical Engineering
Queen's University, Kingston, Ontario Canada K7L 3N6

David J. Thomson
Defence Research Establishment Atlantic
P.O. Box 1012, Dartmouth, Nova Scotia Canada B2Y 3Z7
(April 23, 1998)

Theoretical/numerical models of underwater sound propagation usually incorporate a downgoing radiation condition on the transverse component of the acoustic field. Most one-way or parabolic equation (PE) solvers approximate this radiation condition by appending an absorbing layer to the computational mesh and setting the field to zero at the base of this layer. Papadakis *et al.* [J. Acoust. Soc. Am. **92**, 2030–2038 (1992)] replaced such approximate treatments with a non-local boundary condition (NLBC) that *exactly* transforms the semi-infinite PE problem to an equivalent one in a bounded domain. Papadakis' approach requires the evaluation of a spectral (wavenumber) integral whose integrand is inversely proportional to the impedance of the subbottom medium. In this paper, an alternate procedure is analyzed for obtaining NLBCs directly from the z-space Crank-Nicolson solvers for both the Tappert and Claerbout PEs. Formulas for the field ψ at range $r + \Delta r$ are derived in terms of the known field at the previously calculated range values from 0 to r by expanding the appropriate 'vertical wavenumber' operator for the downgoing field in powers of the translation operator $\mathcal{R} = \exp(-\Delta r \partial_r)$. The effectiveness of these NLBCs are examined for several numerical examples relevant to one-way underwater sound propagation.

For submission to the Journal of the Acoustical Society of America.

Nonlocal boundary conditions for finite-difference parabolic equation solvers[a)]

David Yevick[b)]
Department of Electrical Engineering, Queen's University, Kingston, Ontario K7L 3N6, Canada

David J. Thomson[c)]
Defence Research Establishment Atlantic, P.O. Box 1012, Dartmouth, Nova Scotia B2Y 3Z7, Canada

(Received 10 June 1998; revised 6 April 1999; accepted 12 April 1999)

Theoretical/numerical models of underwater sound propagation usually incorporate a downgoing radiation condition on the transverse component of the acoustic field. Most one-way or parabolic equation (PE) solvers approximate this radiation condition by appending an absorbing layer to the computational mesh and setting the field to zero at the base of this layer. Papadakis *et al.* [J. Acoust. Soc. Am. **92**, 2030–2038 (1992)] replaced such approximate treatments with a nonlocal boundary condition (NLBC) that *exactly* transforms the semi-infinite PE problem to an equivalent one in a bounded domain. Papadakis' approach requires the evaluation of a spectral (wave number) integral whose integrand is inversely proportional to the impedance of the subbottom medium. In this paper, an alternate procedure is analyzed for obtaining NLBCs directly from the z-space Crank–Nicolson solvers for both the Tappert and Claerbout PEs. Formulas for the field ψ at range $r+\Delta r$ are derived in terms of the known field at the previously calculated range values from 0 to r by expanding the appropriate "vertical wave number" operator for the downgoing field in powers of the translation operator $\mathcal{R}=\exp(-\Delta r\partial_r)$. The effectiveness of these NLBCs is examined for several numerical examples relevant to one-way underwater sound propagation. [S0001-4966(99)05207-8]

PACS numbers: 43.30.Bp [SAC-B]

INTRODUCTION

For many applications involving underwater sound propagation, the underlying physics is accurately represented in terms of one-way wave fields that satisfy a parabolic equation (PE). This is convenient, since PEs are amenable to efficient numerical solution by marching algorithms for range-varying as well as range-invariant waveguides (see Ref. 1 and the references therein). Because the ocean subbottom is penetrable to sound waves (particularly at low frequencies), a downgoing radiation condition must be imposed on the transmitted component of the field. In numerical implementations of one-way wave propagation, this condition is usually approximated by appending an *ad hoc* absorbing layer[1–5] to the computational mesh and then applying a local pressure-release boundary condition at the base of the layer. Alternatively, this approximate boundary treatment can be replaced with a nonlocal boundary condition (NLBC) that *exactly* converts the PE problem with a transverse radiation condition at infinity into an equivalent PE problem in a bounded domain.

A nonlocal boundary condition for the standard parabolic equation of underwater acoustics[1,6,7] was first formulated and implemented in a finite-difference PE code by Papadakis.[8] The derivation of Papadakis' result involves transforming the one-way wave equation from coordinate space to the horizontal wave number domain where each spectral component of the PE field ψ satisfies a local impedance boundary condition across the interface $z=z_b$. The transformation back to coordinate space yields a nonlocal boundary condition for ψ, which, for the standard PE, can be cast as a Neumann-to-Dirichlet (NtD) map of the form

$$\psi(r,z_b)=B\int_0^r \psi_z(t,z_b)\frac{\exp[ib(r-t)]}{\sqrt{r-t}}dt. \tag{1}$$

The constants B and b depend on the material properties of the region in the vicinity of $z=z_b$, across which the medium may undergo a jump discontinuity. Equation (1) has been implemented in several applications to underwater acoustics, e.g., Refs. 9–11. This spectral method for obtaining an NLBC was extended by Papadakis[12] to treat the third-order, wide-angle PE of Claerbout,[1,13] which is capable of accommodating wider-angle propagation. Other NLBC forms for use with both standard and/or wide-angle PEs have been derived and implemented for applications in underwater acoustics,[9,14–16] optics,[17,18] radar,[19–21] and atmospheric acoustics.[22,23]

In this paper, we consider an alternative formalism for deriving nonlocal boundary conditions suitable for use with single-term approximations to the PE propagators of one-way waves.[24,25] This method is developed entirely in coordinate space and is specific to finite-difference PE solvers. It is based on the series expansion of a "vertical wave number" operator that arises in identifying the downgoing component of the factored Helmholtz equation in the (uniform) region $z>z_b$. The coefficients that relate the field at range r to the

[a)]Some of the material in this paper was presented at the 133rd meeting of the Acoustical Society of America, 16–20 June 1997, State College, PA.
[b)]Electronic mail: yevick@ibm.net
[c)]Electronic mail: thomson@drea.dnd.ca

 0001-4966/99/106(1)/143/8/$15.00

previously computed values of the field along the boundary are readily obtained by a convolution procedure.

The rest of the paper is organized in the following way. First, we establish the relevant single-term PE approximations for underwater acoustics. Then, we formulate a finite-difference solution procedure which allows us to identify the pseudodifferential equation satisfied by the downgoing wave in $z>z_b$. A nonlocal boundary condition along $z=z_b$ suitable for implementation is obtained by direct expansion of the vertical wave number operator associated with this wave field. We finally demonstrate the effectiveness of such NLBCs for single-term PE propagators by applying them to several test cases relevant to underwater sound propagation.

I. THEORY

A. One-way wave equation

We first construct the one-way propagation equation for a medium with varying density $\rho(z)$ in a region $0<z<z_b$ between the surface ($z=0$) and bottom ($z=z_b$) of a stratified ocean with sound speed and absorption designated by $c(z)$ and $\alpha(z)$, respectively. Since range-varying waveguides are usually modeled as a sequence of range-independent sections, there is no loss of generality in restricting ρ, c, and α in this way. For some reference wave number $k_0=\omega/c_0$, the field ψ can be related to the complex pressure p according to

$$p(r,z)=\frac{\psi(r,z)\exp(ik_0r)}{\sqrt{k_0r}}. \tag{2}$$

Introducing the pseudodifferential operator $\sqrt{1+X}$, where

$$X=N^2-1+k_0^{-2}\rho\frac{\partial}{\partial z}\left(\rho^{-1}\frac{\partial}{\partial z}\right), \tag{3}$$

with $N(z)=n(z)[1+i\alpha(z)]$ and $n(z)=c_0/c(z)$, outgoing propagating waves in the far field ($k_0r\gg1$) can then be described by the formal "one-way" evolution equation[6]

$$\frac{\partial\psi}{\partial r}=ik_0\{-1+\sqrt{1+X}\}\psi. \tag{4}$$

B. Standard PE

To develop a compact form of the nonlocal finite-difference boundary condition that incorporates *a priori* the discrete nature of the propagation problem, we choose to first analyze the standard PE (SPE) of ocean acoustics, which is obtained by approximating the square-root operator in Eq. (3) by

$$-1+\sqrt{1+X}\approx\frac{1}{2}X=\frac{1}{2}(N^2-1)+\frac{1}{2}k_0^{-2}\rho\frac{\partial}{\partial z}\left(\rho^{-1}\frac{\partial}{\partial z}\right). \tag{5}$$

Substituting Eq. (5) into Eq. (4) yields the SPE

$$2ik_0\frac{\partial\psi}{\partial r}+\rho\frac{\partial}{\partial z}\left(\rho^{-1}\frac{\partial\psi}{\partial z}\right)+k_0^2(N^2-1)\psi=0. \tag{6}$$

To generate an NLBC for Eq. (6), we follow Papadakis and simplify the problem further by assuming that the region $z>z_b$ is homogeneous, i.e., one where ρ_b and N_b are constant. Then, for $z>z_b$, Eq. (6) reduces to

$$2ik_0\frac{\partial\psi}{\partial r}+\frac{\partial^2\psi}{\partial z^2}+k_0^2(N_b^2-1)\psi=0. \tag{7}$$

Using the centered finite-difference approximations over the interval from r to $r+\Delta r$

$$\frac{\partial\psi}{\partial r}\approx\frac{\psi(r+\Delta r,z)-\psi(r,z)}{\Delta r}, \tag{8}$$

$$\psi\approx\frac{\psi(r+\Delta r,z)+\psi(r,z)}{2}, \tag{9}$$

results in the implicit Crank–Nicolson formulation of Eq. (7), which we write in the form

$$\left\{k_0^2\nu^2+k_0^2(N_b^2-1)+\frac{\partial^2}{\partial z^2}\right\}\psi(r+\Delta r,z)=\left\{k_0^2\nu^2-k_0^2(N_b^2-1)-\frac{\partial^2}{\partial z^2}\right\}\psi(r,z), \tag{10}$$

where $\nu^2=4i/(k_0\Delta r)$. The goal now is to express the unknown field $\psi(r+\Delta r,z)$ in terms of the known history of field values from $0\rightarrow r$ along the boundary $z=z_b$.

To this end, we introduce the r-space translation operator

$$\mathcal{R}=\exp(-\Delta r\partial_r), \tag{11}$$

and observe that

$$\mathcal{R}^j\psi(r,z)=\psi(r-j\Delta r,z). \tag{12}$$

In terms of $\mathcal{R}$, the Crank–Nicolson representation in Eq. (10) can be cast in the equivalent form as

$$\left\{\frac{\partial^2}{\partial z^2}+\Gamma_0^2\right\}\psi(r+\Delta r,z)=0, \tag{13}$$

where Γ_0 is a z-space vertical wave number operator defined by

$$\Gamma_0^2=k_0^2\left(N_b^2-1+\nu^2\frac{1-\mathcal{R}}{1+\mathcal{R}}\right). \tag{14}$$

Equation (13) can be formally factored into components that govern upgoing and downgoing wave fields. Heuristically, we identify the one-way radiation condition satisfied by the downgoing field at $z=z_b$ as

$$\left\{\frac{\partial}{\partial z}-i\Gamma_0\right\}\psi(r+\Delta r,z_b)=0. \tag{15}$$

A rigorous justification of this step is given elsewhere.[25] When $N_b=1$ in Eq. (14) so that the region $z>z_b$ is lossless and c_0 is chosen equal to c_b, this nonlocal boundary condition reduces to an absorbing boundary condition that is transparent to downgoing waves. Otherwise, it includes those waves that are reflected by the discontinuity in N across the plane $z=z_b$. On the other hand, we can relate Eq. (15) to the exact boundary condition that applies just *inside* the computational region $0<z<z_b$ by making use of the continuity of

pressure and vertical particle velocity across the ocean-bottom interface. Across the plane of discontinuity at $z=z_b$, we immediately find from Eq. (15) that

$$\left.\frac{\partial\psi/\partial z}{\rho_w\psi}\right|_{z_b-0}=\left.\frac{\partial\psi/\partial z}{\rho_b\psi}\right|_{z_b+0}\equiv\frac{i\Gamma_0}{\rho_b}, \tag{16}$$

from which we obtain the required impedance boundary condition

$$\left\{\frac{\partial}{\partial z}-i(\rho_w/\rho_b)\Gamma_0\right\}\psi(r+\Delta r,z_b)=0. \tag{17}$$

Equation (17) accounts for the total impedance jump (sound speed, attenuation, and density) encountered by waves that cross the lower boundary of the waveguide. A numerically tractable, *nonlocal* representation of Eq. (17) results by expanding Γ_0 in a power series in $\mathcal{R}$. This is readily accomplished, for example, by obtaining the Taylor series for the numerator and denominator separately and then convolving the coefficients. Dividing the interval $0\rightarrow r+\Delta r$ into $J+1$ intervals of width Δr and applying the definition of $\mathcal{R}$ from Eq. (12) yields

$$\left\{\frac{\partial}{\partial z}-i\mathcal{B}\right\}\psi[(J+1)\Delta r,z_b]=i\mathcal{B}\sum_{j=1}^{J+1}g_{0,j}\psi[(J+1-j)\Delta r,z_b], \tag{18}$$

where $\mathcal{B}=(\rho_w/\rho_b)k_0\sqrt{N_b^2-1+\nu^2}$. The right-hand side of Eq. (18) is seen to depend solely on the *known* values of the field along the boundary $z=z_b$. This equation allows the boundary value of the acoustic field at the advanced point of a given range-propagation step to be determined in terms of the history of boundary-field values for all previous range steps. The simple analytic nature of this operational procedure, which does not require the evaluation of the inverse Fourier transform of the reciprocal of the impedance spectral function, as in Papadakis' method, allows it to be applied to higher-order PEs in a straightforward way.

C. Wide-angle PE

To extend the above operator formalism to a wider-angle PE, we substitute the [1,1]-Padé approximation for $\sqrt{1+X}$,

$$-1+\sqrt{1+X}\approx\frac{\frac{1}{2}X}{1+\frac{1}{4}X}=\frac{\frac{1}{2}(N_b^2-1)+\frac{1}{2}k_0^{-2}\partial_z^2}{1+\frac{1}{4}(N_b^2-1)+\frac{1}{4}k_0^{-2}\partial_z^2}, \tag{19}$$

into Eq. (4) to obtain Claerbout's rational-linear PE (for $z>z_b$),

$$2ik_0\left\{1+\frac{1}{4}(N_b^2-1)+\frac{1}{4}k_0^{-2}\frac{\partial^2}{\partial z^2}\right\}\frac{\partial\psi}{\partial r}+\frac{\partial^2\psi}{\partial z^2}+k_0^2(N_b^2-1)\psi=0. \tag{20}$$

Applying the same steps leading to Eq. (17) now yields

$$\left\{\frac{\partial}{\partial z}-i(\rho_w/\rho_b)\Gamma_1\right\}\psi(r+\Delta r,z_b)=0, \tag{21}$$

TABLE I. Geoacoustic profile for the Bucker case.

Depth (m)	Sound speed ($m\,s^{-1}$)	Density ($g\,cm^{-3}$)	Attenuation dB λ^{-1}
0	1500	1.0	0.0
120	1498	1.0	0.0
240	1500	1.0	0.0
>240	1505	2.1	0.0

where Γ_1 is a wider-angle vertical wave number operator defined by

$$\Gamma_1^2=k_0^2\left(N_b^2-1+\nu^2\frac{1-\mathcal{R}}{1+\mathcal{R}}\left[1+\frac{1}{4}\nu^2\frac{1-\mathcal{R}}{1+\mathcal{R}}\right]^{-1}\right). \tag{22}$$

After a Taylor series expansion is performed in $\mathcal{R}$, we obtain a nonlocal impedance boundary condition similar to the one given in Eq. (18) but with a new set of coefficients $g_{1,j}$ replacing the $g_{0,j}$ on the right-hand side.

Although it seems reasonable to suppose that the above operator technique can be extended to handle higher-order parabolic equations, such an extension does not appear to be straightforward. In particular, the procedure requires that the downgoing component of the acoustic field be identified in order to construct an appropriate one-way equation similar to Eqs. (17) or (21). Unfortunately, for wide-angle PEs constructed from higher-order Padé approximants, the resulting expression contains nested roots, and the selection of the appropriate root and its subsequent Taylor series evaluation is difficult to determine and implement. Alternatively, multiterm PEs based on Padé and split-step Padé approaches[26,27] can be employed to cast a higher-order PE propagator as a sum of [1,1]-Padé propagators. In this case, the above procedure can in principle be employed to relate the boundary condition after the mth partial step to the previous values of the field at multiple units of the step-length Δr. The main difficulty with this approach is the issue of correctly apportioning the NLBC for the *total* acoustic field into the partial sums.

II. NUMERICAL RESULTS

In this section, we consider three shallow-water propagation examples to demonstrate our numerical implementation of the one-way, nonlocal boundary conditions derived earlier. For each example, the PE+NLBC calculations are based on the Claerbout approximation in Eqs. (20) and (22). Two of the examples involve range-independent waveguides, and for these cases we compare our PE+NLBC results against solutions generated using the wave number integration code SAFARI.[28] For the range-dependent example, we compare our results to solutions produced by the coupled-mode model COUPLE.[29]

The geoacoustic profile for the first example is given in Table I. This range-independent environment exhibits jump discontinuities in both sound speed and density along $z=240$ m. As a result of the small variation in sound speed, only a few normal modes possess real propagation wave numbers. However, the large density jump yields a significant number of virtual modes close to the real wave number

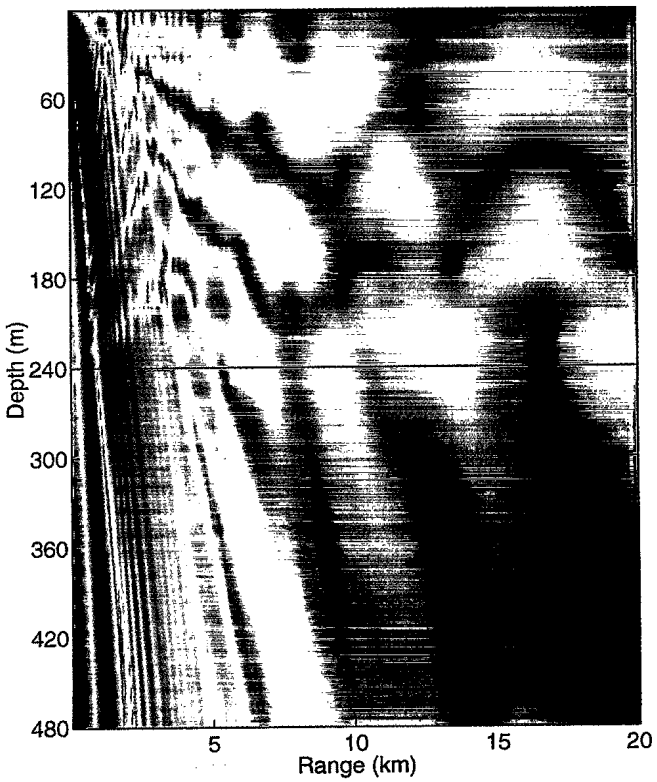

FIG. 1. PE transmission losses for the bilinear profile. The NLBC is applied along $z=480$ m.

axis (Ref. 1, pp. 249–251). This example has been used previously to examine the capability of PE codes for handling density contrasts.[10,30,31] Our focus here, however, is to show that the NLBCs can not only absorb energy that is transmitted into the sea bottom but also account for the reflection/transmission process along the sea-bottom interface. A 100-Hz acoustic source is located at $z=30$ m. For the full-field results shown in Fig. 1, the PE computational grid spanned the domain $0<z<480$ m and the PE solver employed a range step size of $\Delta r=5$ m, a depth step size of $\Delta z=1$ m, and a reference sound speed of $c_0=1500\,\mathrm{m\,s^{-1}}$. The transmission loss levels ($-10\log_{10}|p|^2$) vary from 50 dB (red) to 100 dB (blue). For ranges $r<5$ km, the energy

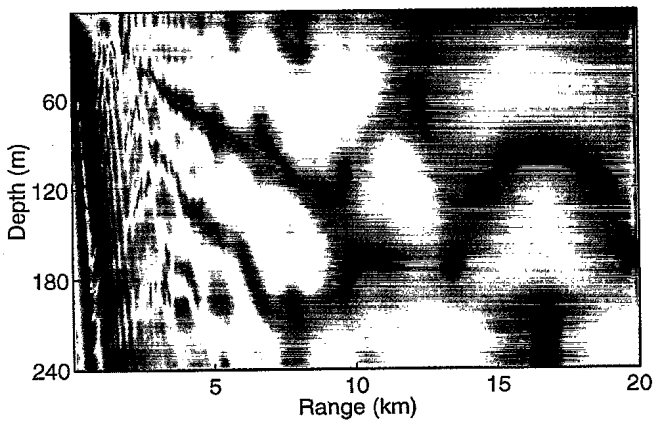

FIG. 2. PE transmission losses for the bilinear profile. The NLBC is applied along $z=240$ m.

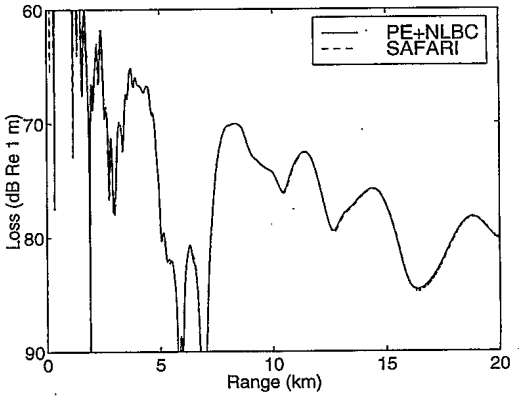

FIG. 3. Transmission loss versus range comparison for the bilinear profile. The receiver depth is $z=90$ m.

clearly undergoes bottom reflection along $z=240$ m, while the slow bottom sound speed allows considerable transmission into the region $z>240$ m. There is no evidence of reflection along $z=480$ m where the NLBC was applied. This indicates that the NLBC successfully annihilates the downgoing energy and behaves as a transparent boundary. Figure 2 shows the results of a calculation in which the computational grid is further reduced to the region $0<z<240$ m. The agreement of the field structure in this figure with the corresponding field of Fig. 1 indicates that the NLBC applied along $z=240$ m correctly handles the reflection and transmission of sound at the sea-bottom interface. When a traditional absorbing layer is used for this example, the computational grid needs to be extended to a depth of $z=2000$ m to adequately suppress reflections. A more detailed depiction of the transmission losses in Fig. 2 is shown in Figs. 3 and 4 for receivers at depths $z=90$ and 240 m, respectively. Also shown in these figures are the reference curves generated using SAFARI. The agreement is observed to be excellent. For this example, the PE calculations obtained with the absorbing bottom required a depth grid 8.3 times larger and executed 1.6 times slower that the PE+NLBC calculations.

Table II lists the geoacoustic profile for the second example, a shallow-water environment that is representative of the southern Mediterranean Sea. The sea bottom is further characterized as an elastic solid with shear speed $c_s=600$ $\mathrm{m\,s^{-1}}$ and shear attenuation $\alpha_s=1.5$ dB λ^{-1}. This configu-

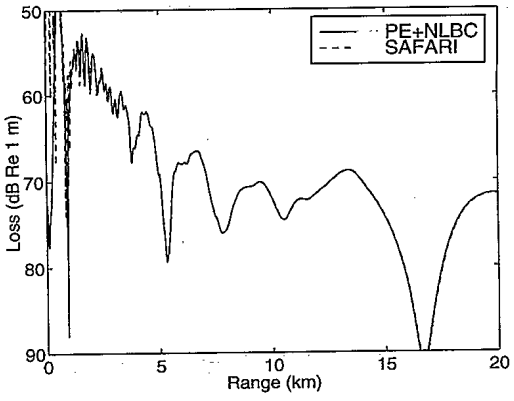

FIG. 4. Transmission loss versus range comparison for the bilinear profile. The receiver depth is $z=240$ m.

TABLE II. Geoacoustic profile for the southern Mediterranean case.

Depth (m)	Sound speed ($m\,s^{-1}$)	Density ($g\,cm^{-3}$)	Attenuation dB λ^{-1}
0.0	1532.8	1.0	0.0
21.1	1531.3	1.0	0.0
22.8	1530.1	1.0	0.0
27.1	1520.1	1.0	0.0
30.1	1518.8	1.0	0.0
46.2	1512.9	1.0	0.0
80.0	1509.0	1.0	0.0
>80.0	1750.0	2.0	0.6

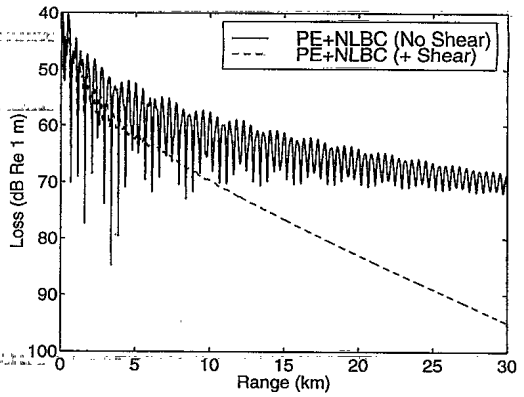

FIG. 5. PE+NLBC transmission loss versus range comparison for the southern Mediterranean profile. The receiver depth is $z=50$ m.

ration was used previously by Bucker[32] to illustrate the effect of a rigid sea bottom on sound propagation. In addition, Bucker showed how the elastic bottom could be approximated with an equivalent fluid which accounts for the extra transmission losses due to shear wave conversion. Bucker's method involves replacing the solid bottom with a stack of sub-bottom acoustic layers having the same density as water but with depth-dependent sound-speed and attenuation profiles. The layer profiles are chosen so that the reflection coefficient R' of the equivalent fluid matches the reflection coefficient R of the true solid near grazing angles that give rise to trapped modes. Recently, Zhang and Tindle[33] introduced an alternative prescription for modeling a solid half space with an equivalent fluid. By a similar matching of reflection coefficients, their method uses the shear parameters of the bottom to transform the true bottom density ρ_b into a complex-valued density ρ_b'. As a result, their method can readily be incorporated into the NLBC formalism introduced in the present paper. This is an alternative to the formally exact spectral approach of combining an acoustic PE with nonlocal boundary conditions to accommodate an elastic bottom.[9,16]

Following Zhang and Tindle, the southern Mediterranean elastic bottom in this paper is modeled with an equivalent fluid having the same compressional sound speed and attenuation as given in Table II but with a complex density given by

$$\rho_b'=\rho_b[(1-2/N_s^2)^2+4i\gamma_s\gamma_b/(k_0^2N_s^4)], \tag{23}$$

where $N_s=(c_0/c_s)(1+i\alpha_s)$. The quantities $\gamma_s=k_0\sqrt{N_s^2-1}$ and $\gamma_b=ik_0\sqrt{1-N_b^2}$ are the vertical wave numbers of the shear and compressional waves in $z>z_b$, respectively. The reference sound speed c_0 can be adjusted within limits to give the best match between R and R' in the vicinity of the propagating modes. The complex density in Eq. (23) is easily incorporated into the NLBCs described earlier via the constant $\mathcal{B}$ in Eq. (18).

Our calculations for this example were carried out at a frequency of 100 Hz for a source and receiver at a depth of 50 m. The NLBC was evaluated along the sea bottom at $z_b=80$ m. The PE computational grid used $\Delta r=10$ m and $\Delta z=0.5$ m. The reflection coefficient of the equivalent fluid was matched to the reflection coefficient of the elastic bottom at a grazing angle of 12 deg, which corresponds to a phase speed of $c_0=1512\,m\,s^{-1}$. Using these parameters, the density of the solid half space is changed from $\rho_b=2\,g\,cm^{-3}$ to $\rho_b'=0.965+0.277i\,g\,cm^{-3}$. To highlight the effect of shear on sound propagation, transmission loss versus range results are shown in Fig. 5 for both the acoustic ($c_s=0$, upper curve) and elastic (lower curve) bottom types. Clearly, the excitation of shear waves in the bottom is a dominant loss mechanism for this particular environment. For comparison to the PE+NLBC results, the corresponding reference values computed using SAFARI are shown in Fig. 6. The PE results are observed to agree well with the SAFARI results for both acoustic and elastic bottom types. The validity of the equivalent fluid approximation is evident in this example. The PE calculations involving an absorbing bottom require that the depth grid be extended to $z=160$ m to achieve stability. In this case, the execution time for the PE +NLBC calculations increased by a factor of 1.4, indicating that the overhead in computing the NLBC convolutions can be significant. Since the number of terms in Eq. (18) increases with increasing range, the marching procedure further slows as the range increases. If the sea bottom is lossy, however, the sums can often be truncated without significant loss of information, but this aspect of the numerical implementation is not pursued in the present paper.

The geoacoustic description for the third example is given in Table III, and corresponds to the deep-end section ($r=0$) of the lossy wedge-test case introduced as one of the Acoustical Society of America (ASA) range-dependent benchmark problems.[26,34,35] Jump discontinuities in sound

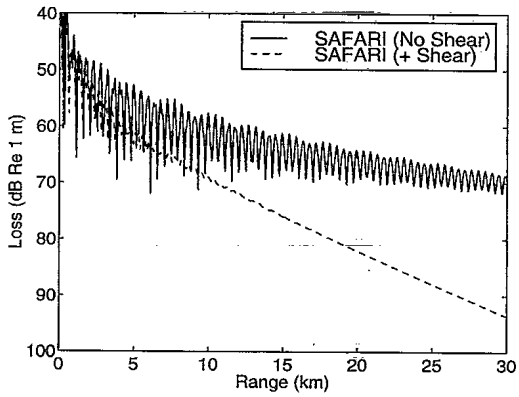

FIG. 6. SAFARI transmission loss versus range comparison for the southern Mediterranean profile. The receiver depth is $z=50$ m.

TABLE III. Deep-end geoacoustic profile for ASA wedge case.

Depth (m)	Sound speed ($m\,s^{-1}$)	Density ($g\,cm^{-3}$)	Attenuation dB λ^{-1}
0	1500	1.0	0.0
200	1500	1.0	0.0
>200	1700	1.5	0.5

speed, density, and absorption occur along the sloping bottom of the wedge, i.e., the line $z=200-r/20$ m. The apex of the wedge is located at $r=4000$ m. A 25-Hz acoustic point source is located at $r=0, z=100$ m.

The standard practice of approximating a range-dependent waveguide by a sequence of range-independent sections and then marching the outgoing field according to a simple range-updating procedure is known to violate energy conservation principles at the vertical interfaces between sections.[36] Several approximate techniques have been developed for ameliorating this difficulty.[37–41] Since our main purpose here is to validate the NLBCs for this range-dependent example, however, we will use a standard staircase approximation and compare our results with those obtained using a false-absorbing bottom. All PE calculations for this example were computed using $\Delta r=5$ m, $\Delta z=0.5$ m, and $c_0=1500\,m\,s^{-1}$.

For the full-field results shown in Fig. 7, the PE computational grid spanned the domain $0<z<250$ m and the NLBC was applied along $z=250$ m. The transmission-loss levels vary from 40 dB (red) to 90 dB (blue). There is no evidence of any sound reflecting from the edge of the computational domain. If the NLBC is replaced with an absorbing layer, the computational grid needs to be extended to a depth of $z=1000$ m to adequately suppress reflections. Transmission losses versus range are compared in Fig. 8 for a receiver at a depth of 30 m. Except at short ranges, the PE+NLBC solution is observed to agree well with the other PE solution which incorporates an absorbing layer in the region $500<z<1000$ m. Corresponding results for a receiver at a depth of 150 m are shown in Fig. 9. Except for the slight differences near the field null at $r\approx3$ km, the curves are in excellent agreement. For this case, the PE+NLBC calculations required only one-quarter of the depth grid of the PE with the absorbing bottom for an equivalent level of accuracy, while the execution time was faster by a factor of 3.9.

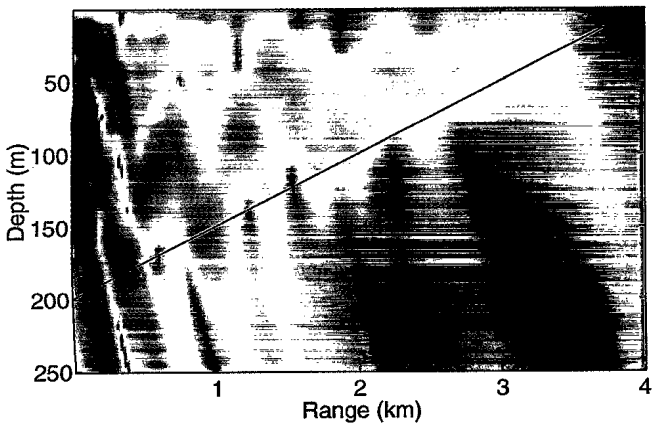

FIG. 7. PE transmission losses for the ASA wedge profile. The NLBC is applied along $z=250$ m.

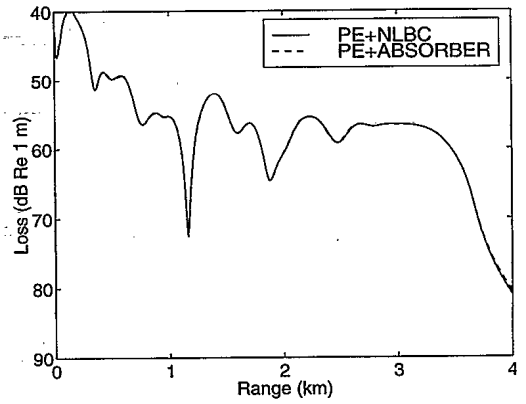

FIG. 8. Transmission loss versus range comparison for the ASA wedge profile. The receiver depth is $z=30$ m.

For this example, the NLBC can also be combined with Collins' rotated PE[37] to yield "two-way" accuracy for the outgoing component of the field by aligning the computational grid with the sloping bottom of the wedge. In rotated coordinates, continuity of pressure and vertical-particle velocity are satisfied naturally along the sea-bottom interface, just as in a range-independent problem. Although the sea surface must now be represented by a staircase boundary, the vanishing of the field on the horizontal steps, in the limit of small vertical steps, is sufficient to approximate the pressure-release boundary condition everywhere. As has been shown elsewhere,[42] by appending a low-impedance air-layer backing to the surface of the wedge, the calculations for the rotated PE may be made to proceed in exactly the same way as for the unrotated PE. In this way, reflection from an external pressure-release boundary is replaced with reflection from an internal fluid/fluid boundary across which the usual boundary conditions apply. The underwater reflection coefficient associated with the water/air boundary should be close to -1.

If we rotate and translate the (r',z') coordinate system about the source position $r=0, z=z_s$, it is convenient to regard r' and z as the independent variables, so that r and z' are determined by

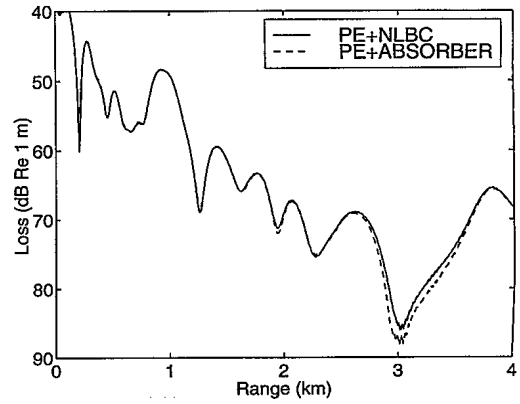

FIG. 9. Transmission loss versus range comparison for the ASA wedge profile. The receiver depth is $z=150$ m.

D. Yevick and

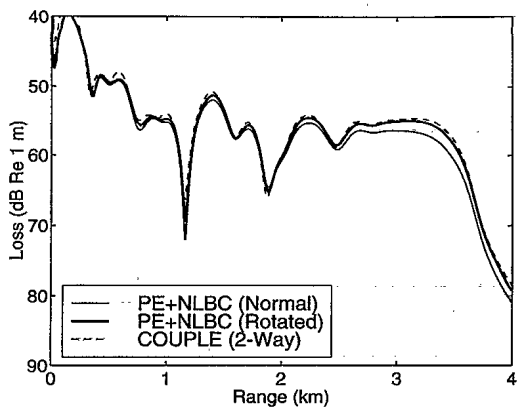

FIG. 10. Transmission loss versus range comparisons for the ASA wedge profile. The receiver depth is $z=30$ m.

$$r+r_0=\frac{r'+z\sin\theta}{\cos\theta},$$
$$z'=(r+r_0)\sin\theta+z\cos\theta. \tag{24}$$

Here, $\theta=\arctan(0.05)\approx 2.86$ deg is the wedge angle and $r_0=z_s\tan\theta=5$ m is the offset along the r-axis. The (r,z')-pairs corresponding to a receiver along $z=30$ m are determined from Eq. (24). The transmission loss versus range curves for the rotated PE with a nonlocal boundary condition (obtained using an air layer with density $\rho_a=0.0012\,\mathrm{g\,cm^{-3}}$, sound speed $c_a=300\,\mathrm{m\,s^{-1}}$, and absorption $\alpha_a=0.5$ dB/λ) and the unrotated (normal) PE with a nonlocal boundary condition are compared in Fig. 10 to reference values generated by COUPLE.[29] It is evident that the rotated PE+NLBC solution does not exhibit the cumulative loss of energy that is evident in the normal PE calculation.

III. CONCLUSIONS

In this paper, we have analyzed an approach to deriving nonlocal boundary conditions (NLBCs) that transforms the semi-infinite PE problem with a radiation condition at infinity into an equivalent PE problem in a bounded domain. In contrast to spectral-based NLBC methods, which require the evaluation of an integral transform from wave number space to physical space, the present algorithm is carried out entirely in the physical domain. It is, however, specific to finite-difference PE solvers as it depends on the series expansion of a vertical wave number operator for the downgoing radiation field in $z>z_b$. By invoking an impedance-continuity condition, we extended this NLBC to a boundary layer at $z=z_b-0$ that separates a uniform half space from the waveguide in $0<z<z_b$ to account for the reflection/transmission process along this (possibly discontinuous) interface. In addition to the standard PE, we similarly derived the NLBC that is appropriate for the Claerbout approximation. Several numerical examples were presented to demonstrate the effectiveness of the NLBC in reducing the computational domain and dispensing with the need for an *ad hoc* absorbing layer. In addition, the equivalent fluid approximation of Zhang and Tindle[33] was shown to be easily incorporated into the NLBC formulation. We conclude that this new nonlocal boundary condition method is an accurate and useful procedure for analyzing paraxial or near-paraxial acoustic-field propagation problems that can be described in the context of single-term approximations to the exact PE propagator.

ACKNOWLEDGMENTS

Financial support for one of us (D.Y.) was provided through the research and development Contract No. W7708–6–0327 with the Esquimalt Defence Research Detachment, a Division of the Defence Research Establishment Atlantic. The same author would like to acknowledge the continued funding provided by the National Research Council of Canada, the Ontario Center for Materials Research, BNR, and Corning Glass.

[1] F. B. Jensen, W. A. Kuperman, M. B. Porter, and H. Schmidt, *Computational Ocean Acoustics* (AIP, New York, 1994), Chap. 6, pp. 343–412.
[2] V. Shevshenko, "The expansion of the fields of open waveguides in proper and improper modes," Radiophys. Quantum Electron. **14**, 972–977 (1974).
[3] J. Bérenger, "A perfectly matched layer for the absorption of electromagnetic waves," J. Comput. Phys. **114**, 185–200 (1994).
[4] D. Yevick, J. Yu, and Y. Yayon, "Optimal absorbing boundary conditions," J. Opt. Soc. Am. A **12**, 107–110 (1995).
[5] D. Yevick, J. Yu, and F. Schmidt, "Analytic studies of absorbing and impedance-matched boundary layers," IEEE Photonics Technol. Lett. **9**, 73–75 (1997).
[6] F. D. Tappert, "The parabolic approximation method," in *Wave Propagation and Underwater Acoustics*, edited by J. B. Keller and J. S. Papadakis (Springer, New York, 1977), Chap. 5, pp. 224–287.
[7] J. A. Davis, D. White, and R. C. Cavanagh, "NORDA Parabolic Equation Workshop, 31 March–3 April 1981," Tech. Note 143, Naval Ocean Research and Development Activity, NSTL Station, MS, 1982; available from NTIS, No. AD-121 932.
[8] J. S. Papadakis, "Impedance formulation of the bottom boundary condition for the parabolic equation model in underwater acoustics," in J. A. Davis, D. White, and R. C. Cavanagh, "NORDA Parabolic Equation Workshop, 31 March–3 April 1981," Tech. Note 143, Naval Ocean Research and Development Activity, NSTL Station, MS, 1982; available from NTIS, No. AD-121 932, p. 83.
[9] J. S. Papadakis, M. I. Taroudakis, P. J. Papadakis, and B. Mayfield, "A New method for a realistic treatment of the sea bottom in the parabolic approximation," J. Acoust. Soc. Am. **92**, 2030–2038 (1992).
[10] D. J. Thomson and M. E. Mayfield, "An exact radiation condition for use with the *a posteriori* PE method," J. Comput. Acoust. **2**, 113–132 (1994).
[11] V. A. Dougalis and N. A. Kampanis, "Finite element methods for the parabolic equation with interfaces," J. Comput. Acoust. **4**, 55–88 (1996).
[12] J. S. Papadakis, "Exact, nonreflecting boundary conditions for parabolic-type approximations in underwater acoustics," J. Comput. Acoust. **2**, 83–98 (1994).
[13] J. F. Claerbout, "Coarse grid calculations of waves in inhomogeneous media with application to delineation of complicated seismic structure," Geophysics **35**, 407–418 (1970).
[14] S. W. Marcus, "A generalized impedance method for application of the parabolic approximation to underwater acoustics," J. Acoust. Soc. Am. **90**, 391–398 (1991).
[15] T. W. Dawson, D. J. Thomson, and G. H. Brooke, "Non-local boundary conditions for acoustic PE predictions involving inhomogeneous layers," in *3rd European Conference on Underwater Acoustics, Vol. 1*, edited by J. S. Papadakis (Crete University Press, Heraklion, 1996), pp. 183–188.
[16] M. E. Mayfield and D. J. Thomson, "An FFT-based non-local boundary condition for the parabolic equation," in *3rd European Conference on Underwater Acoustics, Vol. 1*, edited by J. S. Papadakis (Crete University Press, Heraklion, 1996), pp. 237–242.
[17] V. A. Baskakov and A. V. Popov, "Implementation of transparent boundaries for numerical solution of the Schrodinger equation," Wave Motion **14**, 121–128 (1991).
[18] A. V. Popov, "Accurate modeling of transparent boundaries in quasi-optics," Radio Sci. **31**, 1781–1790 (1996).
[19] S. W. Marcus, "A hybrid (finite-difference–surface Green's function)

method for computing transmission losses in an inhomogeneous atmosphere over irregular terrain," IEEE Trans. Antennas Propag. **40**, 1451–1458 (1992).
[20]M. F. Levy, "Horizontal parabolic equation solution of radiowave propagation problems on large domains," IEEE Trans. Antennas Propag. **43**, 137–144 (1995).
[21]M. F. Levy, "Transparent boundary conditions for parabolic equation solutions of radiowave propagation problems," IEEE Trans. Antennas Propag. **45**, 66–72 (1997).
[22]M. E. Mayfield and D. J. Thomson, "A non-reflecting boundary condition for use in PE calculations of sound propagation in air," J. Acoust. Soc. Am. **92**, 2406 (1992).
[23]R. J. Jardine, W. L. Siegmann, and J. S. Robertson, "Alternative nonreflecting boundary conditions for PE modeling of atmospheric acoustic propagation," in *Environmental Acoustics, Vol. 2,* edited by D. Lee and M. H. Schultz (World Scientific, Singapore, 1994), pp. 849–868.
[24]F. Schmidt and P. Deuflhard, "Discrete transparent boundary condition for the numerical solution of Fresnel's equation," Comput. Math. Appl. **29**, 53–76 (1995).
[25]F. Schmidt and D. Yevick, "Analysis of boundary conditions for the Fresnel equation," J. Comput. Phys. **134**, 96–107 (1997).
[26]M. D. Collins, "Benchmark calculations for higher-order parabolic equations," J. Acoust. Soc. Am. **87**, 1535–1538 (1990).
[27]M. D. Collins, "A split-step Padé solution for the parabolic equation method," J. Acoust. Soc. Am. **93**, 1736–1742 (1993).
[28]H. Schmidt, "SAFARI Seismo-Acoustic Fast field Algorithm for Range-Independent environments," SACLANT Undersea Research Centre, San Bartolomeo, Italy, Rep. SR-113, 1988.
[29]R. B. Evans, "A coupled mode solution for acoustic propagation in a waveguide with a stepwise depth variations of a penetrable bottom," J. Acoust. Soc. Am. **74**, 188–195 (1983).
[30]D. Lee and S. T. McDaniel, "Ocean acoustic propagation by finite-difference methods," Comput. Math. Appl. **14**, 305–423 (1987).
[31]D. Yevick and D. J. Thomson, "A hybrid split-step/finite-difference PE algorithm for variable-density media," J. Acoust. Soc. Am. **101**, 1328–1335 (1997).
[32]H. P. Bucker, "An equivalent bottom for use with the split-step algorithm," J. Acoust. Soc. Am. **73**, 486–491 (1983).
[33]Z. Y. Zhang and C. T. Tindle, "Improved equivalent fluid approximations for a low shear speed ocean bottom," J. Acoust. Soc. Am. **98**, 3391–3396 (1995).
[34]F. B. Jensen and C. M. Ferla, "Numerical solutions of range-dependent benchmark problems in ocean acoustics," J. Acoust. Soc. Am. **87**, 1499–1510 (1990).
[35]D. J. Thomson, "Wide-angle parabolic equation solutions to two range-dependent benchmark problems," J. Acoust. Soc. Am. **87**, 1514–1520 (1990).
[36]M. B. Porter, F. B. Jensen, and C. M. Ferla, "The problem of energy conservation in one-way models," J. Acoust. Soc. Am. **89**, 1058–1067 (1991).
[37]M. D. Collins, "The rotated parabolic equation and sloping ocean bottoms," J. Acoust. Soc. Am. **87**, 1035–1037 (1990).
[38]M. D. Collins and E. K. Westwood, "A higher-order energy-conserving parabolic equation for range-dependent ocean depth, sound speed, and density," J. Acoust. Soc. Am. **89**, 1068–1075 (1991).
[39]M. D. Collins and R. B. Evans, "A two-way parabolic equation for acoustic backscattering in the ocean," J. Acoust. Soc. Am. **91**, 1357–1368 (1992).
[40]D. Lee and W. L. Siegmann, "Finite difference treatment of irregular interfaces: an error analysis," J. Comput. Acoust. **3**, 1–14 (1995).
[41]G. H. Brooke, D. J. Thomson, and P. M. Wort, "A sloping-boundary condition for efficient PE calculations in range-dependent acoustic media," J. Comput. Acoust. **4**, 11–27 (1996).
[42]D. J. Thomson, G. H. Brooke, and E. S. Holmes, "PE approximations for scattering from a rough surface," Defence Research Establishment Pacific, Victoria, B.C., Technical Memorandum 95–21, 1995.